ISSN 2320-2602

International Journal of Advances in Computer Science and Technology (IJACST), Vol.2 , No.11, Pages : 18 - 24

Special Issue of ICCEeT 2013 - Held during 04-05 November, 2013 Dubai

Fractional-order Transmission Line Modeling

R. Ismail[1], R. A. El-Barkouky[2]

[1] German University in Cairo (GUC), Egypt, rawhy.madbouly@guc.edu.eg

[2] Ain Shams University, Egypt, reda_elbarkouky@eng.asu.edu.eg

Abstract: This paper introduces a generalization of the Transmission Line Modeling (TLM) concept in the fractional-order domain. Through this work, the impact of the fractional-order parameters on the TLM properties such as compensation for power loss is shown. Also, it is illustrated how imposing fractional derivatives in the operation of the TLM increases the degree of freedom to control its characteristics, for instance, the scattering matrix. In addition, it is verified that the analysis of the TLM in the conventional case is a special case of the fractional-order study when the fractional-orders equal "1".

Key words : Fractional Calculus, Scattering matrix, transmission Line Modeling (TLM)

INTRODUCTION

Fractional calculus is a branch of mathematical analysis that studies the non-integer differentiation and integration. Although the root of the fractional-calculus was related to the same time-interval of the conventional calculus, but its real revolution appears four decades ago [1-2]. One of the main reasons for this delay is the absence of the real applications that can use it and also due to its complexity relative to the integer-order calculus. After 1960, many papers focus on the approximation and realization of the fractional-element and its advantages [3-5].

There are more than one definition for the fractional differentiation. In particular, the basic definitions of the fractional integral (J^{α}) and fractional derivative (D^{α}) of a function $f(t)$ due to Caputo [1-2] are given by

$$J^{\alpha}f(t) = \frac{1}{\Gamma(\alpha)}\int_0^t (t-\tau)^{\alpha-1} f(\tau)d\tau\,, \quad \alpha \in \mathbb{R}^+, t > 0 \quad \text{(1a)}$$

$$D^{\alpha}f(t) = D^{m}\left(J^{m-\alpha}f(t)\right), \quad m-1 < \alpha \leq m, \quad \text{(1b)}$$

, whereas $m \epsilon N^+$. As shown from the above definition (1) that, the fractional derivative has a global property unlike the conventional derivative. In other words, to calculate the fractional derivative of a certain function $f(t)$ you need to know all the history of this function not only the previous few values as known in the integer-order derivatives. Due to this property, the fractional-order modeling has superior advantages for many physical and natural phenomena which have long-memory dependence better than the conventional integer-order models. In addition, the added parameters (fractional-order α) of the fractional-order systems increases the flexibility and degrees of freedom that can be used for optimizing, best fitting, improving the response….etc.

During the last two decades, numerous systems analysis and generalized theorems based on the fractional-order calculus are introduced mathematically and verified experimentally in different fields such as circuit theory, chemistry, mechanical, control, electromagnetic, and bioengineering [7-18].

It is worth saying that the power dissipated in a circuit modeled by a traditional resistive element is frequency-independent in the conventional case which is really unpractical, especially in high frequencies. However, in the fractional domain the resistive element term is frequency-dependent that is the impedance of a fractional inductor of inductance L and fractional parameter α is given by

$$Z_{Lf} = (j\omega)^{\alpha}L = L\omega^{\alpha}\left[\cos\left(\frac{\pi}{2}\alpha\right) + J\sin\left(\frac{\pi}{2}\alpha\right)\right] \quad (2)$$

, this agrees with experimental results, studies of Coilcraft RF inductors [19] from 1MHz to 1.8 GHz pointed out that the skin effect losses were modeled as $Z(f) = \sqrt{Jf}/H$ which is similar to the half-order inductor.

In the field of electromagnetics, fractional calculus plays an important role. Fractional solutions for the Helmholtz's equation were discussed in [20],[21], the analysis for a homogeneous space which means the geometry of the problem is unbounded was discussed in [20] while different geometries with parallel plane interfaces were considered in [21]. Dedication to studying fractional electromagnetics in fractal spaces is found in [22],[23], whereas Maxwell's equations form in fractal spaces was given in [22], the cylindrical wave equation in fractional dimensional space was solved in [23]. Based on the introduction of the concept of fractional curl operator by N.Engheta [24], several studies were done [25], [26], trying to find a specific fractional solution to a certain electromagnetic problem. This solution is considered as an intermediate one between two given solutions; usually those of the duality principle in electromagnetics, promising results were shown and many publications relied on this concept. In this work, the fractional point of view is befitting from the consideration of fractional time derivatives in the Caputo sense which was not considered in [20]-[26]. Also, all lumped components of the transmission line segments are considered to be fractal ones.

Traditionally, field problems are considerably more difficult to solve than network problems. The transmission-line modeling (TLM), based on Huygens' model [27] of wave propagation and scattering, is a space and time discretizing method for computation of electromagnetic fields based on the analogy between the electromagnetic field and a mesh of transmission lines. In Fig. 1, a simple example of a 2D TLM mesh with a voltage pulse of amplitude 1V incident on the central node is shown. This pulse will be

ISSN 2320-2602
International Journal of Advances in Computer Science and Technology (IJACST), Vol.2 , No.11, Pages : 18 - 24
Special Issue of ICCEeT 2013 - Held during 04-05 November, 2013 Dubai

partially reflected and transmitted according to the transmission-line theory [28] by a factor of half assuming all lines have the same characteristic impedance. The next time step, scattering event excites the neighboring nodes and the process repeats. This paper restudies the TLM in the fractional order sense with all the lumped components considered to be fractal ones.

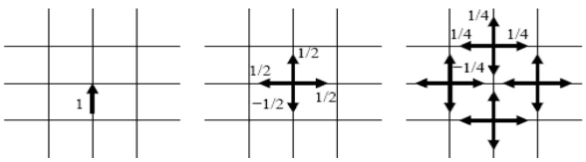

Fig. 1: An example of a 2D TLM mesh

The organization of this paper is as follows: Section 2 shortly reviews an analogy between one-dimensional wave propagation in a lossy medium and a long distributed transmission line. In section 3, spatial sampling and dispersion in the fractional study is discussed showing how to select the sampling length to avoid wave dispersion. The steady state study of the problem is illustrated in section 4 giving the fractional form of the ABCD matrix. As an application, 2D TLM is presented in section 5 giving the fractional scattering matrix. Finally, conclusions are found in section 6.

2. Wave propagation and Transmission Line analogy

Since the lumped components such as L and C were developed to describe the concentrated energy storage in magnetic and electric fields, it is convenient to use them to model fields and as a general case we consider them as fractional elements.

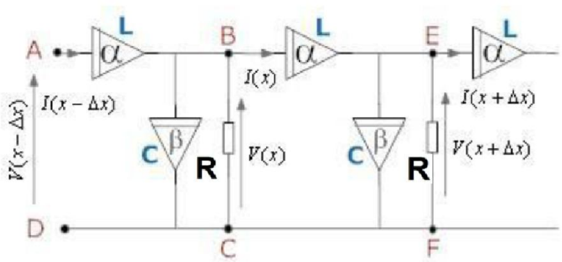

Fig.2: A cascade of segments of a transmission line

Consider a long distributed circuit (a transmission line, TL) as shown in Fig. 2. Following normal practice, the distributed circuit is modeled as a cascade of segments each consists of fractional lumped components L, C with fractional parameters α and β respectively, and a resistor R representing energy storage and dissipation in magnetic and electric fields and with Δx being the length of each segment. Applying Kirchhoff's voltage (KVL) and current (KCL) laws on a segment and assuming $\Delta x \to 0$

$$\frac{\partial^2}{\partial x^2} i(x,t) = \frac{LC}{(\Delta x)^2} \frac{\partial^{\alpha+\beta}}{\partial t^{\alpha+\beta}} i(x,t) + \frac{L}{(\Delta x)^2 R} \frac{\partial^{\alpha}}{\partial t^{\alpha}} i(x,t) \quad (3)$$

Now, consider the propagation of a plane wave along the x-direction in a lossy medium such that

$$E = (0, E_y, 0) \qquad H = (0,0,H_z)$$

then the corresponding Faraday's and Ampere's laws reduce to

$$\frac{\partial^2 E_y(x,t)}{\partial x^2} = \mu\varepsilon \frac{\partial^{\alpha+\beta}}{\partial t^{\alpha+\beta}} E_y(x,t) + \mu\sigma \frac{\partial^{\alpha}}{\partial t^{\alpha}} E_y(x,t) \quad (4)$$

where μ, ε, and σ are, respectively, the magnetic susceptibility, dielectric permittivity, and electric conductivity of the material in which the wave propagates. It is clear that (3) and (4) are similar, which means that there is an analogy between one-dimensional wave propagation in a lossy medium and a long distributed transmission line. This analogy can be extended to two and three dimensions. TLM method uses numerical methods to solve the problem, so discretization is required with respect to both space (segment width Δx) and time (sampling time Δt). The question now is how to determine Δx, certainly the smaller Δx the more accurate solution although small Δx increases the computational time, this is discussed in the following section.

3. Spatial Sampling and Dispersion

From the analogy between (3) and (4) it is noticed that the wave propagates with a velocity $u = \frac{1}{\sqrt{\mu\varepsilon}} = \frac{1}{\sqrt{\frac{L\ C}{\Delta x \Delta x}}}$ which is frequency-independent, however this was deduced based on the assumption that $\Delta x \to 0$ which is unpractical from a computational point of view. Taking into account Δx is very small but not zero, it is expected that u varies with frequency which means that a square pulse, for example, applied on the line will disperse resulting in errors in computations (numerical dispersion). To avoid this, let Δx be very small and look for a condition on it that leads to have an expression for u frequency-independent. Applying KVL to loops ABCDA and BEFCB in Fig. 2 (assuming $R \to \infty$)

$$2v(x,t) - v(x+\Delta x,t) - v(x-\Delta x,t) = L\frac{\partial^{\alpha}}{\partial t^{\alpha}}[i(x,t) - i(x-\Delta x,t)] \quad (5)$$

Applying KCL at node B then,

$$LC\frac{\partial^{\alpha+\beta}}{\partial t^{\alpha+\beta}} v(x,t) = v(x+\Delta x,t) + v(x-\Delta x,t) - 2v(x,t) \quad (6)$$

It is noticed that (6) is a difference equation rather than a differential equation, consider a wave like dependence voltage in the form

$$v(x,t) = v_{max} sin\,(\omega t - kx) \quad (7)$$

where ω is the angular frequency and $k = 2\pi/\lambda$. This source represents a wave propagating with velocity, $u = \omega/k$, substituting (7) in (6) to obtain (see appendix for fractional derivatives of trigonometric functions)

ISSN 2320-2602
International Journal of Advances in Computer Science and Technology (IJACST), Vol.2 , No.11, Pages : 18 - 24
Special Issue of ICCEeT 2013 - Held during 04-05 November, 2013 Dubai

$$\omega^{\alpha+\beta}[sin_{\alpha+\beta}(\omega t-kx)\cos(\alpha+\beta)\frac{\pi}{2} + cos_{\alpha+\beta}(\omega t-kx)\sin(\alpha+\beta)\frac{\pi}{2}] = -4sin^2\left(\frac{k\Delta x}{2}\right)sin\ (\omega t-kx) \quad (8)$$

to simplify dealing with (8), the special case $\alpha+\beta\to 2$ is considered noting that $sin_{\alpha+\beta}(\omega t-kx)\cong sin\ (\omega t-kx)$ as $\alpha+\beta\to 2$, then (8) reduces to

$$\omega^2 LC\ sin(\omega t-kx)\cong 4sin^2\left(\frac{k\Delta x}{2}\right)sin\ (\omega t-kx) \quad (9)$$

therefore

$$\omega^2 = \frac{4}{LC}\ sin^2\left(\frac{k\Delta x}{2}\right) \quad (10)$$

which is not a simple relation between ω and k leading the propagating velocity to be frequency-dependent, to avoid this problem, let's consider

$$\frac{k\Delta x}{2} \ll 1 \quad (11)$$

then $\sin\left(\frac{k\Delta x}{2}\right)\cong\frac{k\Delta x}{2}$ and consequently $\frac{\omega}{k}=\frac{\Delta x}{\sqrt{LC}}$ which coincides with the continuous case, therefore the numerical dispersion is negligible and the discrete network is an acceptable representation of the actual system. Errors are always present but by using fine enough discretization, such errors are minimized. It should be noted that a useful "rule of thumb" is that

$$\Delta x\le\frac{\lambda}{10} \quad (12)$$

4. ABCD MATRIX OF A TL IN THE FRACTIONAL CASE

Consider again the TL segment shown in Fig. 2. Now, we discuss the steady state condition, Applying KVL and taking limit as $\Delta x\to 0$

$$\frac{dV}{dx} = -I(x)Z_{Lf} \quad (13a)$$

where $Z_{Lf}=(j\omega)^{\alpha}L_d$ is the fractional impedance of the inductor with L_d is inductance of the TL per unit length. Applying KCL with $\Delta x\to 0$

$$\frac{dI}{dx} = -V(x)Y_{Cf} \quad (13b)$$

where $Y_{Cf}=(j\omega)^{\beta}C_d$ is the fractional admittance of the capacitor with C_d is capacitance of the TL per unit length. From (13a) and (13b), it is easy to deduce that

$$\frac{d^2V}{dx^2}-\gamma^2V(x)=0 \quad (13c)$$

where γ is the propagation constant, $\gamma^2=Z_{Lf}Y_{Cf}$

$$\gamma=\sqrt{L_dC_d}\ \omega^{\frac{\alpha+\beta}{2}}[cos\frac{(\alpha+\beta)\pi}{2}+jsin\frac{(\alpha+\beta)\pi}{2}\ ] \quad (14)$$

the real part of the propagation constant γ represents the attenuation constant and hence it is important to check its sign, noticing (14) and as practically $0<\alpha,\beta<2$, it is easy to deduce the region of α and β for the attenuation constant to be negative which is $1<\alpha+\beta<3$,

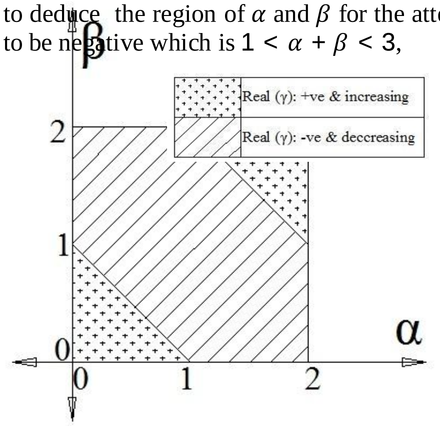

Fig.3: $Re(\gamma)$ versus α and β

Fig. 3 illustrates the region at which the attenuation constant is whether positive or negative, decreasing or increasing as a function of ω for fixed α and β. Solving (13c) to find $V(x)$ and consequently $I(x)$, the following formula is obtained to relate the signals at a distance l to those at the starting point on the line

$$\begin{bmatrix}V(0)\\I(0)\end{bmatrix}=\begin{bmatrix}\cosh(\gamma l) & \frac{Z_{Lf}}{\gamma}\sinh(\gamma l)\\ \frac{\gamma}{Z_{Lf}}\sinh(\gamma l) & \cosh(\gamma l)\end{bmatrix}\begin{bmatrix}V(l)\\I(l)\end{bmatrix} = \begin{bmatrix}A & B\\C & B\end{bmatrix}\begin{bmatrix}V(l)\\I(l)\end{bmatrix} \quad (15)$$

The characteristic impedance of the transmission line (Z_f) is determined as

$$Z_f=\sqrt{\frac{Z_{Lf}}{Y_{Cf}}}=\sqrt{\frac{(j\omega)^{\alpha}L_d}{(j\omega)^{\beta}C_d}}=(j\omega)^{\frac{\alpha-\beta}{2}}\sqrt{\frac{L_d}{C_d}} \quad (16)$$

therefore $\frac{Z_{Lf}}{\gamma}=Z_f$. Now (15) becomes

$$\begin{bmatrix}V(0)\\I(0)\end{bmatrix}= \begin{bmatrix}\cosh(\gamma l) & Z_f\sinh(\gamma l)\\ \frac{1}{Z_f}\sinh(\gamma l) & \cosh(\gamma l)\end{bmatrix}\begin{bmatrix}V(l)\\I(l)\end{bmatrix} \quad (17)$$

The determinant of the ABCD matrix $\Delta=cosh^2(\gamma l)-sinh^2(\gamma l)=1\neq 0$, therefore this matrix is nonsingular. Setting all fractional derivatives equal one in the ABCD matrix, the conventional case is retrieved [27]. It is noticed that the ABCD matrix in the fractional study is complex valued elements rather than the conventional study, this is can be seen that imposing fractional parameters compensates

ISSN 2320-2602
International Journal of Advances in Computer Science and Technology (IJACST), Vol.2 , No.11, Pages : 18 - 24
Special Issue of ICCEeT 2013 - Held during 04-05 November, 2013 Dubai

for losses, also imposing fractional parameters in this matrix gives more degrees of freedom in the study of TLM.

Equation (16) gives a formula for the characteristic impedance of the TL in the fractional case at which it is complex, it may be important to check the sign of its real part (the resistive element) which is affected by the difference between the fractional parameters α and β. Fig. 4 illustrates the different regions in the $\alpha-\beta$ plane at which $Re(Z_f)$ whether positive or negative, decreasing or increasing as a function of ω.

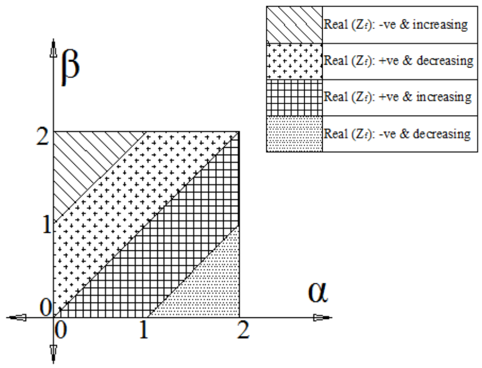

Fig.4: $Re(Z_f)$ versus α and β.

The input impedance Z_{in} of the transmission line is given by

$$Z_{in} = \frac{V(0)}{I(0)} \qquad (18a)$$

Substituting $V(0)$ and $I(0)$ from (17) and replacing $I(l)$ by $\frac{V(l)}{Z_1}$, where Z_1 is the impedance of the load connected at the end of the line, then

$$\frac{Z_{in}}{Z_f} = \frac{\frac{Z_1}{Z_f} + \tanh(\gamma l)}{1 + \frac{Z_1}{Z_f}\tanh(\gamma l)} \qquad (18b)$$

Fig. 5 (a), (b), and (c) demonstrate $Re(Z_{in}), Im(Z_{in})$ and $|Z_{in}|$ as a function in $(\alpha-\beta, \alpha+\beta)$ at $Z_1 = 20 + 20J\ \Omega$, $\omega = 1GHz$, $\sqrt{\frac{L_d}{C_d}} = 50$, it is shown that Z_{in} has significant values near the region $\alpha-\beta > 1.5$ at which $|Z_{in}|$ is an increasing function of the fractional parameters $(\alpha-\beta, \alpha+\beta)$, also the conventional case is retrieved at $(\alpha-\beta, \alpha+\beta) = (0,2)$. Setting $Z_1 \to \infty$ in (18b) it is obtained

$$Z_{in} = \frac{Z_f}{\tanh(\gamma l)} \qquad (19a)$$

however, $\tanh(\gamma l) = \frac{\tan(j\gamma l)}{j}$, if the length l is much smaller than the wavelength then $\tan(j\gamma l) \approx j\gamma l$ and therefore

$$Z_{in} \cong \frac{Z_f}{\gamma l} = \frac{(j\omega)^{\frac{\alpha-\beta}{2}}\sqrt{\frac{L_d}{C_d}}}{l\sqrt{L_d C_d}(j\omega)^{\frac{\alpha+\beta}{2}}} = \frac{1}{(j\omega)^{\beta} C_d l} \qquad (19b)$$

this indicates that a short in length TL segment with an open circuit at the far end may be viewed as a small fractional capacitor. Similarly, by putting $Z_1 = 0$ in (18b) as a TL segment with a short circuit at BB an inductor is modeled,

$$Z_{in} = (j\omega)^{\alpha} L_d l \qquad (19c)$$

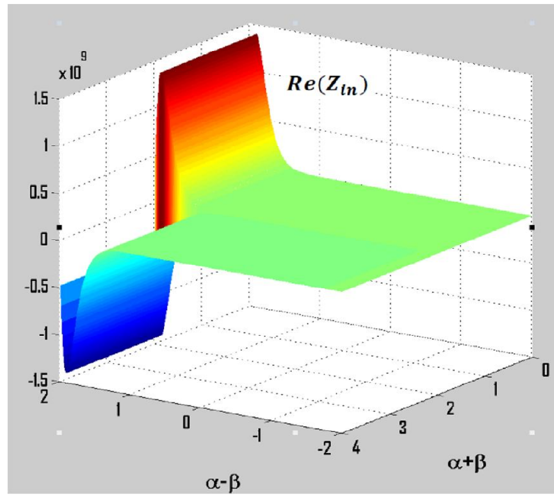

Fig. 5(a)

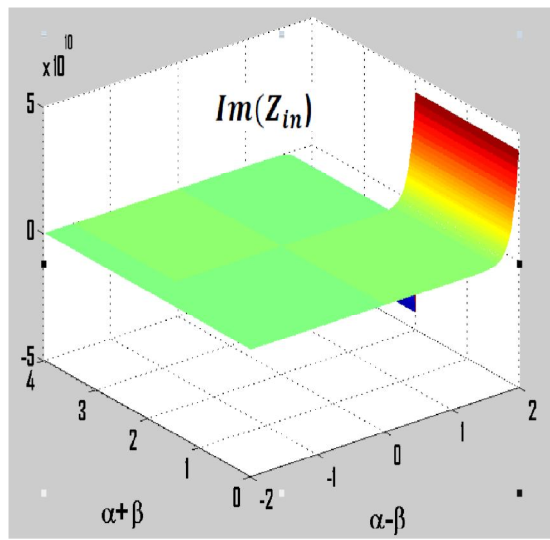

Fig. 5(b)

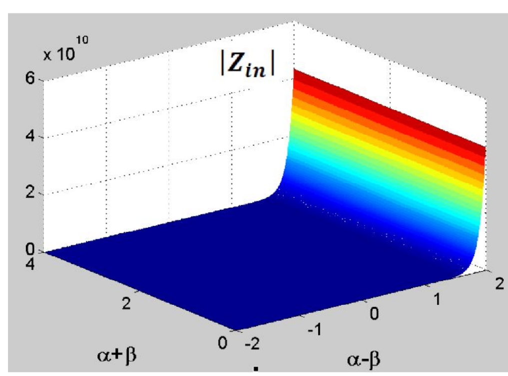

Fig. 5(c)

Fig. 5: Z_{in} versus $(\alpha-\beta)$ and $(\alpha+\beta)$

ISSN 2320-2602
International Journal of Advances in Computer Science and Technology (IJACST), Vol.2 , No.11, Pages : 18 - 24
Special Issue of ICCEeT 2013 - Held during 04-05 November, 2013 Dubai

During the charging process of a TL half the energy of the source is stored in the inductance in a form of a magnetic field while the other half is stored in the form of an electric field in the capacitance. If the end terminal of the TL segment is an open circuit leading to a zero current, the energy stored in the inductance is transferred to the capacitance resulting the voltage to be doubled. This helps to construct the equivalent Thevenin circuit looking at the port BB shown in Fig. 6b [27] with v^i is the incident voltage at BB. This circuit is valid for a time interval τ, that is after time interval τ a new pulse v^i from the source is imposed.

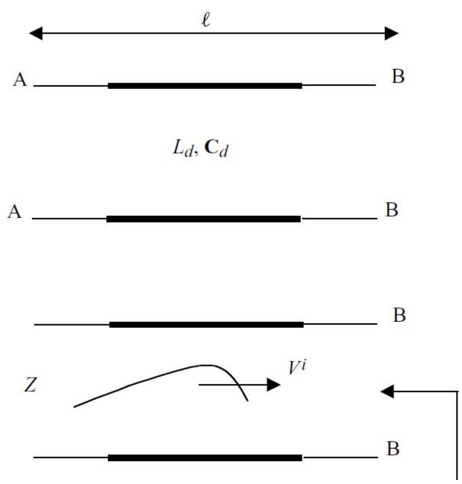

Fig.6a: a TL segment with a voltage pulse V^i propagating towards BB

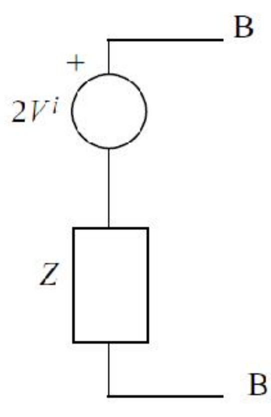

Fig.6b: Thevenin equivalent circuit seen at BB

5. Two Dimensional TLM

As an application, consider two intersecting TLs of the same length as shown in Figs. 7a, 7b [27]. Assume that Z_{fx} and Z_{fy} are the characteristic impedances along the horizontal and vertical TLs, respectively, with

$$Z_{fx} = \sqrt{\frac{L_d}{C_d}}(j\omega)^{\gamma_x}, Z_{fy} = \sqrt{\frac{L_d}{C_d}}(j\omega)^{\gamma_y} \qquad (20)$$

where $\gamma_x = \frac{\alpha_x - \beta_x}{2}, \gamma_y = \frac{\alpha_y - \beta_y}{2}$. Actually, there are two arrangements of 2D TLs "series" (Fig. 7a) and "shunt" (Fig. 7b), in this paper we focus on the series node arrangement..The entire problem space is a replication of Fig. 7a in each direction, according to Huygen's principal each pulse reflected from the node impinges on the adjacent node and sets up a spherical wave. The pulses associated with that wave become incident on the adjacent nodes to set up more spherical waves, i.e. pulses propagate and scatter in the grid of lines as being the modeling medium. Assume that $\Delta x = \Delta y = \Delta l$ where the choice of Δl is dependent on the spatial resolution required and the shortest wavelength in use and as pointed above $\Delta l < \lambda/10$ for accuracy.

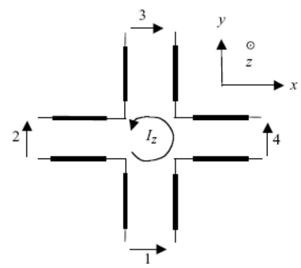

Fig.7a: Series TLM node

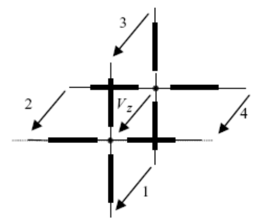

Fig.7b: Shunt TLM node

The basic operation of the 2D TLM is as follows. At each node and at each time step k there are four incident pulses which generate four reflected pulses after scattering at the node (scattering process). These pulses propagate out of each node to become incident on the adjacent nodes at the next time step $k+1$ (connection process) and the process repeats. An observer at node (x, y, z) can replace what he or she sees by the Thevenin equivalent circuit shown in Fig. 8, accordingly, the loop current at time step k is then

$$_kI_z = \frac{2\,_kV_1^i + 2\,_kV_4^i - 2\,_kV_2^i - 2\,_kV_3^i}{2Z_{fx} + 2Z_{fy}} \qquad (21)$$

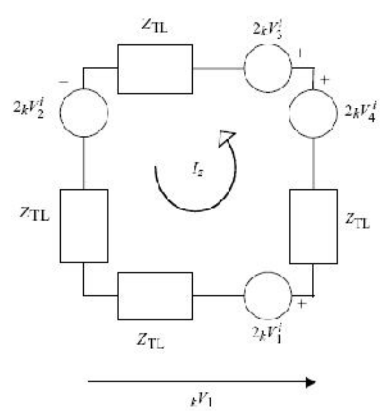

Fig.8: Thevenin equivalent circuit of a series node

where $_kV_j^i$ is the incident voltage at node j at time step k, the voltage across node 1 at time step k is then

$$_kV_1 = 2\,_kV_1^i - \,_kI_zZ_{fy} \qquad (22a)$$

where the reflected voltage from node 1 at time step k is determined as

$$_kV_1^r = \,_kV_1 - \,_kV_1^i \qquad (22b)$$

ISSN 2320-2602
International Journal of Advances in Computer Science and Technology (IJACST), Vol.2 , No.11, Pages : 18 - 24
Special Issue of ICCEeT 2013 - Held during 04-05 November, 2013 Dubai

Substituting from (22a) and (22b) in (21) yields

$$ {}_kV_1^r = \frac{1}{(j\omega)^{\gamma_x} + (j\omega)^{\gamma_y}}\left((j\omega)^{\gamma_x}\,{}_kV_1^i + (j\omega)^{\gamma_y}\,{}_kV_2^i + (j\omega)^{\gamma_y}\,{}_kV_3^i - (j\omega)^{\gamma_y}\,{}_kV_4^i\right) \qquad (22c)$$

Similarly, ${}_kV_2^r$, ${}_kV_3^r$, ${}_kV_4^r$ can be obtained in terms of ${}_kV_1^i$, ${}_kV_2^i$, ${}_kV_3^i$ and ${}_kV_4^i$. The scattering process can be expressed in terms of a scattering matrix S, as

$$ {}_kV^r = S\;{}_kV^i \qquad (23)$$

where

$$ {}_kV^r = [\,{}_kV_1^r \;\; {}_kV_2^r \;\; {}_kV_3^r \;\; {}_kV_4^r]^T $$
$$ {}_kV^i = [\,{}_kV_1^i \;\; {}_kV_2^i \;\; {}_kV_3^i \;\; {}_kV_4^i]^T $$

where superscript T stands for transpose,

$$ S = \frac{1}{(j\omega)^{\gamma_x}+(j\omega)^{\gamma_y}}\left[(j\omega)^{\gamma_x}\begin{pmatrix} 1 & 0 & 0 & 0\\ 1 & 0 & -1 & 1\\ 0 & 0 & 1 & 0\\ -1 & 1 & 1 & 0\end{pmatrix} + (j\omega)^{\gamma_y}\begin{pmatrix} 0 & 1 & 1 & -1\\ 0 & 1 & 0 & 0\\ 1 & -1 & 0 & 1\\ 0 & 0 & 0 & 1\end{pmatrix}\right]. \qquad (24\text{-a})$$

Putting $\gamma_x = \gamma_y = 0$ then

$$ S = 0.5\begin{pmatrix} 1 & 1 & 1 & -1\\ 1 & 1 & -1 & 1\\ 1 & -1 & 1 & 1\\ -1 & 1 & 1 & 1\end{pmatrix} \qquad (24b)$$

at which the conventional case is retrieved. In the conventional case the scattering matrix is pure real rather than in the fractional case, that is again fractional compensates for losses. Now, equations (23) and (24a) represent the scattering process at each node.

6. Conclusion

The analogy between the electromagnetic field and a mesh of transmission lines was restudied considering the lumped components to be fractional which is more realistic. This analogy enables us to solve a network problem rather than a field problem known as TLM. Using numerical methods to solve the problem, there is an upper bound for the segment width to avoid wave dispersion. It was noticed that the ABCD and the scattering matrices in the fractional study are complex valued elements rather than the conventional study; this gives more degrees of freedom in the study of TLM to control its characteristics. Also this is can be seen that imposing fractional parameters compensates for power losses. The conventional case is easily retrieved by setting all fractals to one.

Appendix

Fractional Derivatives of Trigenometric Functions

Define the following function E_μ^t

$$ E_\mu^t = D^\mu(e^t) = D^\mu\left(\sum_{k=0}^{\infty}\frac{t^k}{k!}\right) = \sum_{k=0}^{\infty}\frac{t^{k-\mu}}{\Gamma(k+1-\mu)} $$

Accordingly,

$$ E_0^t = e^t\,, D^\mu(e^{at}) = a^\mu E_\mu^{at} $$

Define also the generalized trigonometric functions

$$ cos_\mu t = \frac{1}{2}\left(E_\mu^{it} + E_\mu^{-it}\right) = \sum_{k=0}^{\infty}\frac{t^{k-\mu}}{\Gamma(k+1-\mu)}\cos\left((k-\mu)\frac{\pi}{2}\right) $$

$$ sin_\mu t = \frac{1}{2i}\left(E_\mu^{it} - E_\mu^{-it}\right) = \sum_{k=0}^{\infty}\frac{t^{k-\mu}}{\Gamma(k+1-\mu)}\sin\left((k-\mu)\frac{\pi}{2}\right) $$

This leads to the generalized Euler relation

$$ E_\mu^{it} = cos_\mu t + i sin_\mu t $$

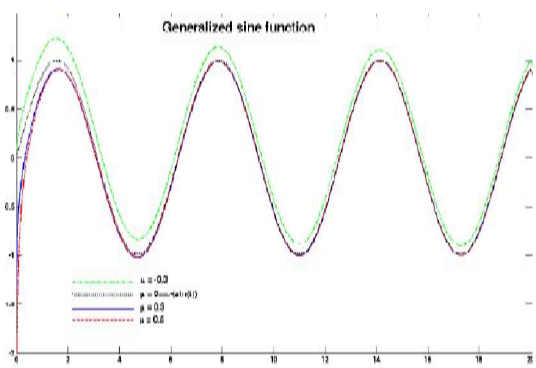

Integer derivative of the generalized functions

$$ Dcos_\mu t = -sin_\mu t + \frac{\cos\left(\frac{\mu\pi}{2}\right)}{\Gamma(-\mu)\,t^{\mu+1}} \quad , $$

$$ \lim_{t\to\infty}(Dcos_\mu t) = -sin_\mu t \cong -sint $$

$$ Dsin_\mu t = cos_\mu t - \frac{\sin\left(\frac{\mu\pi}{2}\right)}{\Gamma(-\mu)\,t^{\mu+1}} \quad , $$

$$ \lim_{t\to\infty}(Dsin_\mu t) = cos_\mu t \cong cost $$

Fractional derivative of the original functions

$$ D^\mu sin\; t = \frac{1}{2i}\left(D^\mu e^{it} - D^\mu e^{-it}\right) = \frac{1}{2i}\left(e^{i\mu\frac{\pi}{2}}E_\mu^{it} - e^{-i\mu\frac{\pi}{2}}E_\mu^{-it}\right) $$

$$= sin_{\mu}t \quad cos(\tfrac{\mu\pi}{2}) + cos_{\mu}t \quad sin(\tfrac{\mu\pi}{2})$$

Similarly,

$$D^{\mu}cos\ t = \frac{1}{2}(D^{\mu}e^{it} + D^{\mu}e^{-it}) = \frac{1}{2}(e^{i\mu\frac{\pi}{2}}E_{\mu}^{it} + e^{-i\mu\frac{\pi}{2}}E_{\mu}^{-it})$$

$$= cos_{\mu}t \quad cos(\tfrac{\mu\pi}{2}) - sin_{\mu}t \quad sin(\tfrac{\mu\pi}{2})$$

REFERENCES

[1] S. G. Samko, A. A. Kilbas and O. I. Marichev, *Fractional integrals and derivatives: theory and application*, Gordon & Breach, 1987.

[2] J. Sabatier, O.P. Agrawal and J.A. Tenreiro Machado, *Advances in fractional calculus; theoretical developments and applications in physics and engineering*, Springer, 2007.

[3] G. Carlson, and C. Halijak, "Approximation of fractional capacitors (1/s)1/n by a regular Newton process, " *IEEE Trans. Circuits &Syst*, 11, 210-213, 1964.

[4] M. Nakagawa, and K. Sorimachi, "Basic characteristics of a fractance device," *IEICE Trans. Fundam. Electron. Commun. Comput. Sci.*, vol. E75, no.12, pp. 1814-1819, 1992.

[5] T. C. Haba, G. L. Loum, G. Ablart, "An analytical expression for the input impedance of a fractal tree obtained by a microelectronical process and experimental measurements of its non-integral dimension," *Chaos, Solitons and Fractals*, 33, 364–373, 2007.

[6] KostadinTrenˇcevski, ˇZivoradTomovski, "On fractional derivatives of some functions of exponential type", *Univ. Beograd. Publ. Elektrotehn.* Fak., Ser. at. 13 (2002), 77–84.

[7] R. L. Magin, *Fractional calculus in bioengineering*, Begell House, Connecticut, 2006.

[8] C.C. Tseng and S.L. Lee, "Design of Fractional-order Digital Differentiator Using Radial Basis Function," *IEEE Trans. Circuits & Syst.*-I, vol. 57, no. 7, 391- 404, 2010

[9] C. M. Ionescu and R. De Keyser, "Relations between Fractional-order Model Parameters and Lung Pathology in Chronic Obstructive Pulmonary Disease," *IEEE Trans. On Biomedical Eng.*, vol. 56, no. 4, 978- 987, 2009.

[10] R. Martin, J. J. Quintara, A. Ramos and L. De La Nuez, " Modeling electrochemical double layer capacitor, from classical to fractional impedance," *Journal of Computational and Nonlinear Dynamics*, vol. 3, no. 2, 2008.

[11] I. S. Jesus, T. J. A. Machado and B. J. Cunha, "Fractional electrical impedances in botanical elements," *Journal of Vibration and Control*, vol. 14, no. 9-10, pp.1389-1402, 2008.

[12] G. W. Bohannan, S. K. Hurst, and L. Springler, "Electrical component with fractional-order impedance," *Utility Patent Application*, US20060267595, 2006.

[13] P. Melchior, B. Orsoni, O. Lavialle, and A. Oustaloup, "The CRONE toolbox for Matlab: fractional path planning design in robotics, *Laboratoire d'Automatiqueet de Productique* (LAP) 2001. John Wiley & Sons, Ltd. Int. J. Circ. Theor. Appl. 2008.

[14] A. G. Radwan, A. S. Elwakil, and A. M. Soliman, "Fractional-order Sinusoidal Oscillators: Design Procedure and Practical Examples," *IEEE Trans. Circuits & Syst.*-I, vol. 55, pp. 2051-2063, 2008.

[15] A. G. Radwan, A. S. Elwakil, and A. M. Soliman, "On the generalization of second-order filters to fractional-order domain," *Journal of Circuits Systems & Computers*, vol. 18, no. 2, pp.361-386, 2009.

[16] A. G. Radwan, A. M. Soliman , A. S. Elwakil, and A. Sedeek, "On the stability of linear systems with fractional-order elements," *Chaos, Solitons& Fractals*, vol. 40, 5, 2317-2328, 2009.

[17] A. Shamim, A. G. Radwan, K. N. Salama, "Fractional Smith Chart Theory and Application," *IEEE Microwave and Wireless Components Letters*, vol. 21, 3, 117- 119, 2011.

[18] A. G. Radwan, A. Shamim, K. N. Salama, "Theory of Fractional-order Elements Based Impedance Matching Networks," *IEEE Microwave and Wireless Components Letters*, vol. 21, 3, 120- 122, 2011.

[19] Modeling Coilcraft RF Inductors. *Coilcraft Document* 158 May 1999 [Online].Available: http://www.coilcraft.com

[20] N. Engheta,"Use of Fractional Integration to Propose Some ``Fractional" Solutions for the Scalar Helmholtz Equation", *Progress In Electromagnetics Research*, PIER 12, 107-132, 1996.

[21] Q. A. Naqvi and A. A. Rizvi, "Fractional Solutions for the Helmholtz's Equation in a Multilayered Geometry", *Progress In Electromagnetics Research, PIER* 21, 319-335, 1999.

[22] M. Zubair, M. J. Mughal, Q. A. Naqvi, and A. A. Rizvi, "Differential Electromagnetic Equations in Fractional Space", *Progress In Electromagnetics Research, PIER* 114, 255-269, 2011

[23] M. Zubair, M. J. Mughal, and Q. A. Naqvi ,"An Exact Solution of the Cylindrical Wave Equation for Electromagnetic Field in Fractional Dimensional Space", *Progress In Electromagnetics Research, PIER* 114, 443-455, 2011.

[24] Engheta, N., "Fractional curl operator in electromagnetics," *Microwave and Optical Technology Letters*, Vol. 17, No. 2, 86–91, 1998.

[25] A. Hussain, S. Ishfaq, and Q. A. Naqvi,"Fractional Curl Operator and Fractional Waveguides", *Progress In Electromagnetics Research, PIER* 63, 319-335, 2006.

[26] M. Faryad and Q. A. Naqvi , "Fractional Rectangular Waveguide", *Progress In Electromagnetics Research, PIER* 75, 383-396, 2007.

[27] Christos Christopoulos, *The Transmission-Line Modeling (TLM) Method in Electromagnetics*, Morgan & Claypool publisher, 2006.

[28] M.N.O. Sadiku, *Elements of Electro-magnetics*, 5th edition, Oxford University Press, 2010.